Journal of Neonatal Surgery
ISSN(Online): 2226-0439
Vol.14 , Issue 32s (2025)
https://www.jneonatalsurg.com

OPEN ACCESS

Formulation, Statistical Optimization And In Vitro Ex Vivo Characterization Of Enteric Coated Nanocarriers For Enhanced Oral Bioavailability Of A Bio-Pharmaceutically Challenged Drug

Subhranshu Panda[1], Shubham Tikait[2*], Swati Deshmukh[3]

[1]Director, School of Pharmaceutical Sciences, Jaipur National University (JNU), Jaipur, Rajasthan-302017

[2*]Research Scholar, Jaipur National University (JNU), Jaipur, Rajasthan-302017

[3]Principal, Shraddha Institute of pharmacy (SIOPs), Washim, Maharashtra-444505

Corresponding Author,

Shubham Tikait,

Research Scholar, Jaipur National University, Jaipur, Rajasthan-302017

Email: shubhamtikait004@gmail.com

.Cite this paper as: Subhranshu Panda, Shubham Tikait, Swati Deshmukh (2025 Formulation, Statistical Optimization And In Vitro Ex Vivo Characterization Of Enteric Coated Nanocarriers For Enhanced Oral Bioavailability Of A Bio-Pharmaceutically Challenged Drug. Journal of Neonatal Surgery, 14, (32s) 10555-10570

ABSTRACT

Rifaximin, a Biopharmaceutics Classification System (BCS) Class II drug, exhibits poor aqueous solubility and limited systemic bioavailability following oral administration. The present study aimed to develop and optimize rifaximin-loaded enteric-coated solid lipid nanoparticles (RFN-EC-SLN) to enhance its oral absorption and therapeutic performance. A Quality by Design (QbD)-based Box–Behnken Design (BBD) approach was employed to optimize formulation variables, including lipid, surfactant, and polymer concentrations, with particle size, entrapment efficiency, and drug release as critical quality attributes.

The optimized formulation (F6) demonstrated a mean particle size of 154 ± 2.6 nm, PDI of 0.21 ± 0.03, zeta potential of +17.5 ± 0.04 mV, and high entrapment efficiency (82.0 ± 1.6%). In vitro release studies revealed minimal drug release under gastric conditions (pH 1.2) and sustained release up to 86.0 ± 2.4% at intestinal pH (6.8), following zero-order kinetics (R^2 = 0.989). Stability studies conducted under accelerated conditions confirmed the physicochemical stability of the formulation.

Acute toxicity evaluation in Wistar rats showed no mortality, behavioral abnormalities, or significant hematological and biochemical alterations, confirming systemic safety. Pharmacokinetic studies demonstrated significantly enhanced absorption of the SLN formulation, with increased Cmax, nearly two-fold higher AUC, prolonged half-life, and relative bioavailability of 159.3% compared to conventional rifaximin suspension.

Overall, the developed enteric-coated SLN system effectively improved the solubility, intestinal protection, and oral bioavailability of rifaximin, highlighting its potential as a promising delivery platform for biopharmaceutically challenged drugs..

Keywords: *Rifaximin; Solid lipid nanoparticles; Enteric coating; Eudragit L100; Box–Behnken design; Quality by Design; Oral bioavailability; Controlled release; Pharmacokinetics; BCS Class II drug.*

INTRODUCTION

Oral drug delivery continues to be the most preferred route of administration because of its convenience, patient compliance, cost-effectiveness, and overall safety profile. Despite these advantages, many therapeutic agents categorized under the Biopharmaceutics Classification System (BCS) Class II demonstrate limited aqueous solubility, which significantly compromises their dissolution rate, intestinal absorption, and ultimately their bioavailability. Rifaximin, a poorly water-soluble antimicrobial agent characterized by minimal systemic absorption, exemplifies this challenge. Although primarily intended for localized action within the gastrointestinal tract, its therapeutic efficiency remains constrained by inadequate solubility and suboptimal release behavior.1

Recent progress in nanotechnology has enabled the development of advanced carrier systems aimed at overcoming solubility-related limitations. Among these, solid lipid nanoparticles (SLNs) have emerged as a promising approach for enhancing the oral delivery of poorly soluble drugs. SLNs are composed of physiologically compatible lipids and stabilizing agents,

providing advantages such as improved drug solubilization, enhanced stability, sustained release characteristics, and potential site-specific delivery. For lipophilic molecules like rifaximin, incorporation into SLNs facilitates improved dispersion within gastrointestinal fluids, thereby promoting enhanced drug performance.2

However, nanoparticulate systems administered orally are still exposed to the harsh acidic environment of the stomach, which may induce premature drug release or degradation.[3] To address this limitation, enteric coating strategies employing pH-sensitive polymers such as Eudragit® L100 have been widely explored. These polymers remain intact under acidic gastric conditions but dissolve at higher intestinal pH, enabling targeted drug release in the small intestine while reducing gastric irritation.[3] Furthermore, formulation components such as glyceryl monostearate, serving as the lipid matrix, and Pluronic F68, functioning as a stabilizing surfactant, play crucial roles in maintaining structural integrity, improving dispersibility, and enhancing formulation efficiency.[4-5]

In this context, the present investigation aims to formulate, optimize, and comprehensively evaluate enteric-coated solid lipid nanocarriers of rifaximin to improve its solubility and oral bioavailability. The developed formulations were characterized with respect to particle size, zeta potential, entrapment efficiency, drug loading capacity, *in-vitro* drug release, and enteric protection performance. Through systematic optimization and *in vitro–ex vivo* assessment, the study seeks to establish an efficient nanocarrier platform for enhancing the oral delivery of biopharmaceutically challenged drugs.

MATERIALS AND METHODS:

Rifaximin as a gift sample from Chief Pharmaceuticals Ltd., China. Glyceryl monostearate (GMS) and Eudragit L100 were procured from Loba Chemie and Evonik India Pvt. Ltd., respectively. Pluronic F68 was sourced from Sigma-Aldrich, USA. All solvents and reagents used I this research purchased from Merck Mumbai.

Preformulation studies:

Determination of Maximum Wavelength (λmax) [6]

A stock solution of Rifaximin was prepared by dissolving a deliberated quantity in methanol to obtain a conc. of 100 µg/mL. This solution was then diluted to 10 µg/mL for UV-Visible spectrophotometric analysis. The sample was scanned over a wavelength range of 300 to 600 nm using methanol as the blank. The wavelength showing maximum absorbance was identified and recorded as the λmax for Rifaximin.

Preparation of Calibration Curve[7]

A calibration curve was constructed using standard solutions of Rifaximin in methanol at conc. of 2, 4, 6, 8, and 10 µg/mL. The abs. of each solution was measured at the previously determined λmax. A plot of absorbance (AU) versus concentration (µg/mL) was generated, and a linear regression equation was calculated to determine the correlation coefficient (R^2) and assess the linearity of the method.

FTR Spectroscopy[8]

FTIR spectroscopy was directed to investigate potential interactions between Rifaximin and formulation excipients. Samples of pure Rifaximin were prepared by triturating with potassium bromide (KBr) in a 1:100 ratio. The resulting pellets were scanned using an FTIR spectrophotometer (e.g., Bruker or PerkinElmer) in the range of 4000–400 cm^{-1}.

DSC Study[9]

DSC analysis was employed to assess thermal behaviour and drug-excipient compatibility. Approximately 2–5 mg of Rifaximin were weighed accurately and sealed in standard aluminum pans. The samples were heated from 30°C - 300°C at a rate of 10°C/min under a constant nitrogen purge. The thermograms were recorded using a calibrated DSC instrument (DSC 4000, PerkinElmer).

Preparation of Rifaximin-Loaded Enteric-Coated Solid Lipid Nanoparticles (RFN-EC-SLN) [10-12]

RFN-EC-SLN was prepared using the solvent injection method. Glyceryl monostearate (lipid phase) was dissolved in 5 mL of ethanol and melted in a water bath. Rifaximin (20 mg) was added to the molten lipid and sonicated for 1 minute using a probe sonicator (Qsonica Q500, USA). The aqueous phase (10 mL) containing Pluronic F68 was homogenized at 3000 rpm for 1 hour, into which the lipid solution was slowly injected. The resulting dispersion was ultracentrifuged at 10,000 rpm for 30 minutes to collect lipid aggregates. These aggregates were re-dispersed in 10 mL of aqueous polyvinyl alcohol solution and stirred at 1000 rpm for 3 hrs. to form a uniform precipitate. For enteric coating, the precipitate was suspended in 10 mL of Eudragit L100 buffer (pH 6.8) and agitated at 1000 rpm for 2 hours, followed by probe sonication for 10 minutes. The final suspension formulation was centrifuged at 10 thousand rpm for 30 min. and freeze-dried to obtain RFN-EC-SLN.

Design and Optimization of RFN-EC-SLN Using Box-Behnken Design (BBD) [11-13]

The preparation of rifaximin-loaded enteric-coated solid lipid nanoparticles (RFN-EC-SLN) was carried out through a Quality by Design (QbD)-guided strategy employing the BBD statistical model, executed using Design Expert software (version 13.0, Stat-Ease, USA). Three independent formulation variables-lipid concentration (factor A), surfactant concentration (factor B), and polymer amount (factor C) were investigated at three coded levels (−1, 0, +1). The dependent

outcome variables selected for optimization were particle size (response Y1), entrapment efficiency (response Y2), and percentage drug release (response Y3).

Characterization RFN-EC-SLN formulation:

Particle Size, PDI, and Zeta Potential Analysis [14]

The average particle size, size distribution (PDI), & zeta potential of RFN-EC-SLN formulation were analyzed (Zetasizer Nano ZS). PDI values indicated the uniformity of the nanoparticles, while zeta potential measurements served as predictors of colloidal stability based on electrostatic repulsion.

Entrapment Efficiency and Drug Content[15]

Encapsulation efficiency was determined by centrifuging 1 mL of the nanoparticle suspension (1 mg/mL drug) at 15,000×g for 30 min. at 4 °C. The supernatant was diluted with methanol, and the drug content was quantified using UV–Visible spectrophotometry at 296 nm.

pH Measurement[16]

The pH of the optimized formulation was determined at 37 °C using a calibrated digital pH meter (Ohaus ST10 Pen Meter). For direct measurement, the electrode was carefully immersed into the nanoparticle dispersion, ensuring values reflected physiologically relevant conditions.

Scanning Electron Microscopy (SEM)[17]

The external morphology of RFN-EC-SLN was visualized using SEM (JEOL JMS-7400, Japan). A drop of the sample was applied to a silicon wafer, dried at 25 °C, and observed under high-resolution imaging to assess shape and surface characteristics.

Transmission Electron Microscopy (TEM)[18]

TEM analysis (JEOL 1230, USA) was performed to examine the internal structure and nanocarrier shape. Diluted RFN-EC-SLN was dropped onto 300-mesh copper grids, dried, and visualized under high magnification for structural evaluation.

***In-Vitro* Drug Release Study**[19]

Drug release from the optimized RFN-EC-SLN was studied using dialysis cassettes (MWCO 2,000 Da). The formulation was exposed to simulated gastric fluid (pH 1.2) for 2 hours, followed by transfer to simulated intestinal fluid (pH 6.8) for 22 hours. Samples collected at intervals were analyzed by UV spectrophotometry to calculate cumulative release.

Stability Studies[20-21]

Accelerated stability testing was performed as per ICH Q1A (R2) guidelines in a chamber set at 40 ± 2 °C/75 ± 5% RH for three months. Formulations were periodically evaluated for drug content, particle size, PDI, zeta potential, and physical appearance to confirm stability under stress conditions.

Statistical Analysis[22]

Each experiment was performed in triplicate, and the findings are expressed as mean values with their corresponding standard deviations. Data interpretation and statistical validation were carried out using GraphPad Prism software (version 10.0).

***In vivo* pharmacological evaluation**

Healthy wistar albino rats (150–200 g) were obtained from a CPCSEA-registered facility and maintained under standardized laboratory conditions (23 ± 2°C; 55–65% relative humidity; 12-hour light/dark cycle). Animals were acclimatized for one week with free access to standard pellet diet and water. Prior to dosing, rats were fasted overnight while water was provided ad libitum. All experimental procedures were performed in accordance with IAEC approval and CPCSEA guidelines.[23-26]

Acute toxicity and safety assessment

Acute oral toxicity was conducted following OECD guideline 423 to evaluate the short-term safety profile of Rifaximin formulations. Eighteen rats were randomly divided into three groups (n = 6): oral Rifaximin suspension, oral Rifaximin-loaded SLN formulation, and intravenous Rifaximin solution. Oral groups received a limit dose of 2000 mg/kg, while the IV group was administered the highest feasible safe dose. Animals were closely observed for the first 4 hours post-administration and subsequently monitored daily for 14 days for signs of toxicity, behavioural changes, or mortality. Body weight was recorded on days 0, 7, and 14. At study completion, haematological parameters (haemoglobin, RBC, WBC, PCV, platelets) and biochemical markers (AST, ALT, ALP, bilirubin, creatinine, urea, BUN) were analyzed to assess systemic safety.[27-38]

Preparation of test formulations

The oral rifaximin suspension was prepared by dispersing finely powdered tablets in 0.5% w/v carboxymethyl cellulose (CMC) solution and was freshly prepared before administration. The optimized Rifaximin-loaded SLN formulation was

reconstituted in distilled water and vortexed to ensure uniform dispersion prior to oral dosing. For intravenous administration, rifaximin was solubilized using sterile water containing PEG-400 and polysorbate 80, followed by centrifugation and filtration through a 0.22 µm membrane under aseptic conditions. Drug concentration was verified before dosing.[39-40]

Pharmacokinetic study design

A controlled comparative pharmacokinetic study was performed using three groups (n = 6 per group). Group E1 received oral rifaximin suspension (20 mg/kg), group E2 received oral Rifaximin-loaded SLN equivalent to 20 mg/kg rifaximin, and group E3 received intravenous rifaximin at 20 mg/kg. All animals were fasted overnight before dosing. Oral formulations were administered by gavage, while intravenous dosing was performed via the lateral tail vein under aseptic conditions.[41-43]

Blood sampling and plasma analysis

Serial blood samples (~0.3 ml) were collected via retro-orbital puncture under light anaesthesia at predefined intervals. For oral groups, samples were collected at 0, 0.25, 0.5, 1, 2, 4, 6, 8, 12, and 24 hours, whereas for the iv group, sampling was performed at 0, 0.08, 0.25, 0.5, 1, 2, 4, 6, 8, and 12 hours. Blood samples were centrifuged at 5000 rpm for 10 minutes to separate plasma, which was stored at −20°C until analysis[44-45]

Plasma Rifaximin concentrations were determined using a validated reverse-phase HPLC method employing a C18 column with a methanol: water (70:30 v/v) mobile phase. Detection was carried out at 296 nm, and calibration curves in the range of 5–30 µg/ml demonstrated acceptable linearity ($r^2 > 0.99$).[46-47]

Pharmacokinetic and statistical analysis

Pharmacokinetic parameters were calculated using non-compartmental analysis, including maximum plasma concentration (Cmax), time to reach peak concentration (tmax), area under the curve (auc_{0-24} and $auc_{0-\infty}$), elimination half-life ($t_{½}$), and elimination rate constant (kel). Relative bioavailability of oral formulations was estimated using the IV group as reference. All results were expressed as mean ± SD. Normality was assessed using the shapiro–wilk test and intergroup comparisons were performed using one-way ANOVA followed by tukey's post HOC test. A value of $P < 0.05$ was considered statistically significant. Statistical analysis was conducted using validated software (graph pad prism V9.0 or equivalent).[48-50]

RESULT AND DISCUSSIONS:

Maximum Wavelength Detection

The UV-Visible spectrophotometric analysis of Rifaximin revealed that the drug exhibited its maximum absorbance at **337 nm**. This wavelength corresponds to the point of highest absorption in the scanned range, making it the most suitable for quantitative estimation. The λmax was determined by scanning a diluted solution of Rifaximin between 300 to 600 nm using methanol as a blank.

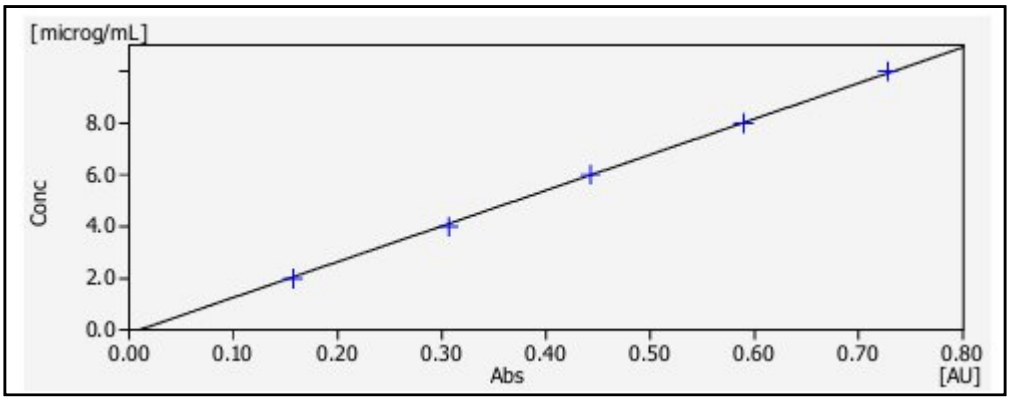

Fig. 1: Calibration curve of Rifaximin in methanol (Absorbance vs. Concentration)

Calibration Curve of Rifaximin

The calibration curve for Rifaximin was constructed using standard solutions ranging from 2 to 10 µg/mL in methanol. Absorbance values were recorded at 337 nm. A linear regression analysis was performed, yielding the equation:

Absorbance = 0.0742 × Concentration + 0.0531

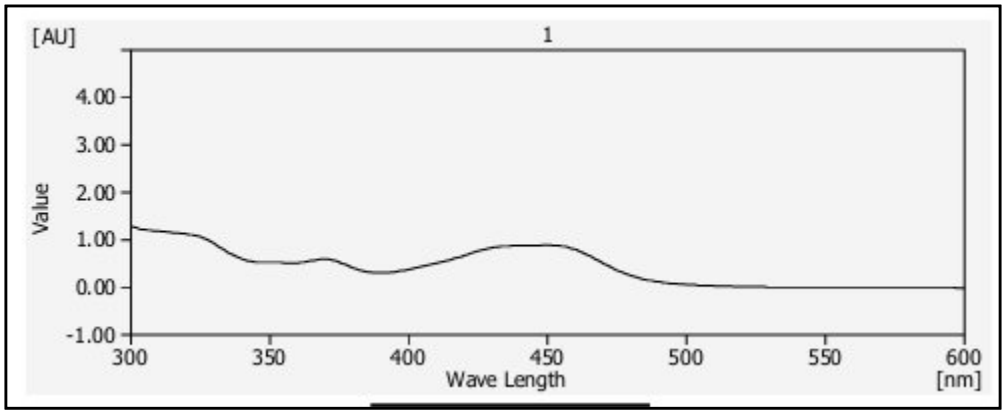

Fig. 2: UV spectrum of Rifaximin showing peak absorbance around 337 nm

FTIR Spectra of Rifaximin

The FTIR spectrum of Rifaximin confirmed the presence of its characteristic functional groups, indicating structural stability and purity. A broad absorption band at 3402.86 cm^{-1} corresponds to O–H stretching, signifying hydrogen-bonded hydroxyl groups. Peaks at 3075.15 cm^{-1} indicate aromatic C–H stretching, while absorptions at 2928.59 and 2863.56 cm^{-1} represent aliphatic C–H stretching. A sharp peak at 1664.15 cm^{-1} confirms the C=O stretching of ketone and lactone groups, crucial for the drug's antibacterial activity. Additionally, the C–O–C stretch observed at 1050.42 cm^{-1} suggests the presence of ether, ester, and lactone functionalities. The absence of unexpected peaks or significant shifts supports the chemical integrity and compatibility of Rifaximin.

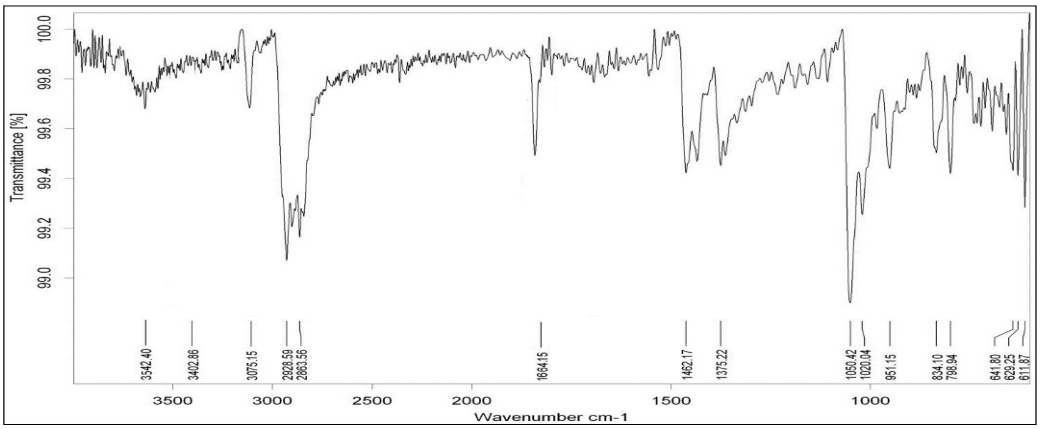

Fig. 3: FTIR Spectra of Rifaximin

DSC Thermogram of Rifaximin

The DSC of the Rifaximin was carried out by using instrument. The peak of Rifaximin was observed on the 202.08°C which is in the standard range of 200–205°C which confirms the presence of Rifaximin.

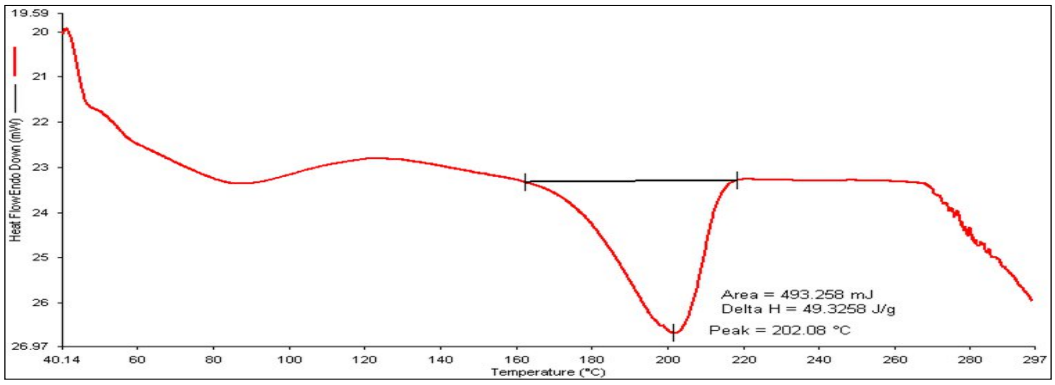

Fig. 4: DSC thermogram of pure drug Rifaximin

Design and optimization of RFN-EC-SLN using QbD-based BBD approach

Thirteen RFN-EC-SLN formulations (F1–F13) were developed using the solvent injection method and optimized using the BBD under the QbD framework. The study evaluated the influence of 3 independent variables lipid concentration (A), surfactant (B), and enteric polymer (C) on particle size (Y1), entrapment efficiency (Y2), and drug release (Y3). The lipid content ranged from 50–150 mg, surfactant from 200–600 mg, and enteric polymer (Eudragit L100) from 40–80 mg. The optimization aimed to meet the Quality Target Product Profile (QTPP). Statistical analysis revealed that variables A (lipid) and C (enteric polymer) significantly influenced all three responses ($p < 0.05$), while surfactant concentration (B) had minimal impact. The regression model demonstrated a good fit, with experimental values aligning well with predicted outcomes. The derived polynomial equations confirmed lipid concentration as the most influential factor, with the highest positive coefficient values for particle size (+205 nm), EE (+73%), and drug release (+78%). This highlights the lipid phase's critical role in determining nanoparticle characteristics and guiding formulation optimization.

Table 1: Optimization of Rifaximin-loaded enteric-coated solid lipid nanoparticles (RFN-EC-SLN) formulation

Formulation	Drug	Formulation factors			Responses		
		Conc. of Lipid (mg)	Conc. of Surfactant (mg)	Conc. polymer (mg)	Particle size (nm)	Entrapment efficiency (%)	Drug release (%)
F1	20	50	600	60	152	72	84
F2	20	50	200	60	192	67	75
F3	20	50	400	80	182	75	78
F4	20	50	400	40	174	66	87
F5	20	100	200	40	168	74	82
F6	***20***	***100***	***600***	***40***	***154***	***82***	***86***
F7	20	100	600	80	185	82	75
F8	20	100	400	60	205	73	78
F9	20	100	200	80	210	77	69
F10	20	150	200	60	351	71	72
F11	20	150	600	60	248	80	74
F12	20	150	400	80	319	78	69
F13	20	150	400	40	295	76	76

Table 2: Independent Variables levels used in BBD for RFN-EC-SLN optimization

Independent Variables	Level used, actual coded		
	Low (-1)	Medium (0)	High (+1)
A= Lipid: Glyceryl monostearate (mg)	50	100	150
B= Surfactant: Pluronic F68 (mg)	200	400	600
C= Polymer: Eudragit L100 (mg)	40	60	80

Characterization RFN-EC-SLN formulation:

Particle Size

Particle size analysis provides critical insight into the physical characteristics of the developed nanosystem. The optimized

RFN-EC-SLN formulation shows a mean particle size of 154 ± 2.6 nm, indicating nanoscale dispersion ideal for enhancing gastrointestinal absorption. The increased surface area of these nanoparticles supports efficient systemic delivery by promoting faster dissolution and uptake.

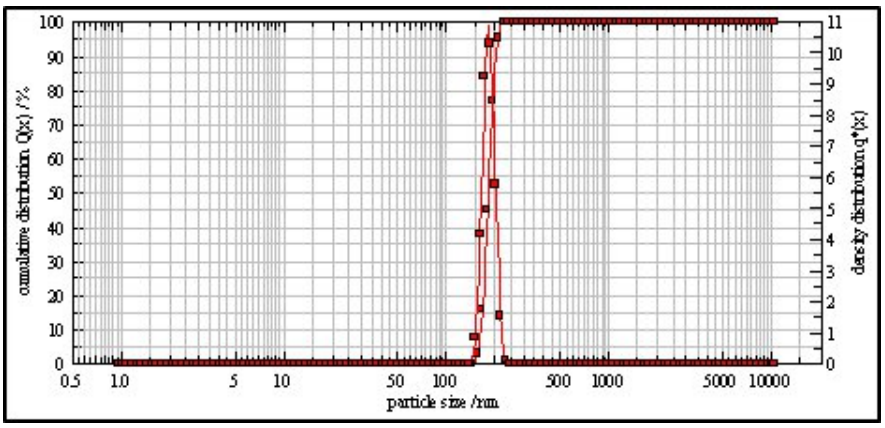

Fig. 5: Particle size of optimized RFN-EC-SLN formulation

Polydispersity Index (PDI)

The Polydispersity Index (PDI) was found to be 0.21 ± 0.03, suggesting a narrow and uniform size distribution of the nanoparticles. A lower PDI value reflects a homogeneous population of nanoglobules, which is essential for minimizing the risk of aggregation and ensuring formulation stability.

Zeta Potential

The zeta potential was measured at +17.5 ± 0.04 mV for optimized formulation. This positive surface charge can be recognized to the presence of cationic components such as Eudragit L100.

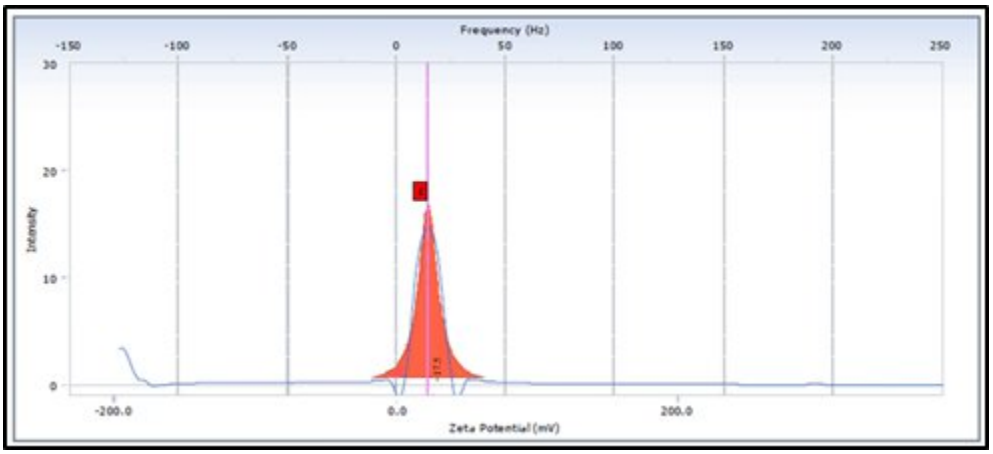

Fig. 6: Zeta potential of RFN-EC-SLN Formulation

Entrapment Efficiency (EE %)

The EE% and drug content of the RFN-EC-SLN formulation were assessed to determine the formulation's drug-loading capacity. The formulation exhibited an entrapment efficiency of 82.0 ± 1.6%, indicating successful incorporation of rifaximin within the solid lipid nanoparticle matrix. The drug loading was found to be 10.2 ± 0.2%, confirming the nanosystem's potential as an effective delivery carrier.

Drug Content

These values suggest that the selected formulation components including the lipid matrix, polymer coating, and surfactant system were well-suited for efficiently encapsulating rifaximin. High entrapment and drug-loading capacities are vital for enhancing oral bioavailability, reducing dosing frequency, and improving therapeutic outcomes.

pH Analysis

The pH of the RFN-EC-SLN formulation was determined to be 6.9 ± 0.2, falling within the acceptable range for oral pharmaceutical preparations (pH 2–9). This pH value closely aligns with the physiological pH of the oral cavity (typically between 6.2 and 7.6), indicating that the formulation is unlikely to cause mucosal irritation or discomfort upon oral

administration.

Maintaining a physiologically compatible pH is essential for patient compliance and safety, as it supports the stability and acceptability of the formulation during transit through the gastrointestinal tract.

Table 3: Physico-chemical characterization of RFN-EC-SLN

Formulation	Physicochemical Properties					
	Globule size (nm)	PDI	Zeta potential (mV)	EE (%)	RFN loading (%)	pH
RFN-EC-SLN	154 ± 2.6	0.21 ± 0.03	+17.5 ± 0.04	82.0 ± 1.6	10.2 ± 0.2	6.9 ± 0.2

Surface Morphology by SEM & TEM

The morphology of the RFN-EC-SLN was examined using SEM, which was discovered to have spherical shape nanoparticles. Particle diameter was determined to be compatible with particle size measurements, and no particle aggregation was seen in the SEM pictures. Additionally, SEM examination demonstrated a homogeneous distribution of spherical particles, which aligned with the microscopy study.

The TEM imaging method was used to examine the internal diameter and morphology of the developed RFN-EC-SLN. It was discovered to be spherical in shape and had a 160 nm diameter. Given that both methods support and validate the nanoscale size of the RFN-EC-SLN particles, the results demonstrated a strong correlation between the DLS and TEM data. As a result, TEM measurements confirm that the nanosystem is distributed uniformly.

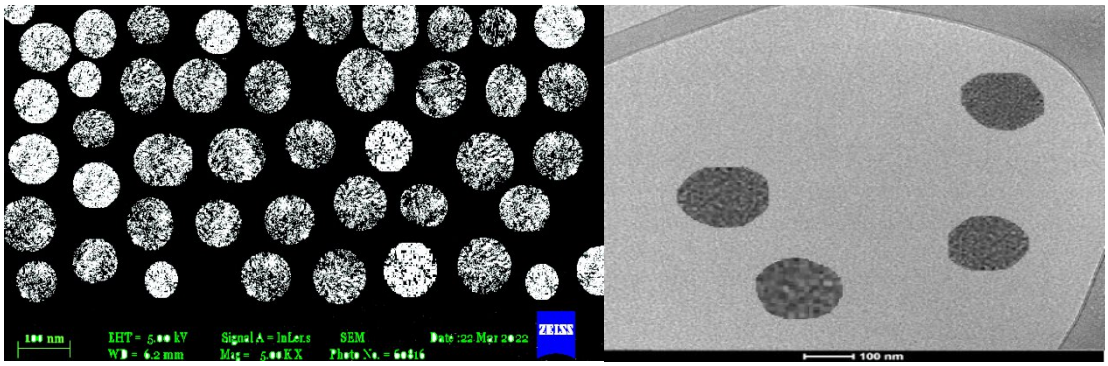

(B)

Fig. 7: Surface morphology examination of RFN-EC-SLN by (A) SEM and (B) TEM

***In-vitro* Drug Release Studies**

Among total 13 formulations, formulation F6 was identified as the most promising based on optimization criteria suggested by the Box–Behnken Design (BBD) and design expert analysis. The release profile of RFN from the optimized RFN-EC-SLN formulation (F6) was assessed using dialysis cassettes with a M.W. cut-off of 2,000 Da. In simulated gastric fluid (pH 1.2), the formulation exhibited a limited release of 15.8 ± 3.4% RFN over the initial 2 hours, demonstrating gastric resistance. When transitioned to simulated intestinal fluid (pH 6.8), a sustained release pattern was observed, with cumulative RFN release reaching 86.0 ± 2.4% over 24 hours.

Regression analysis indicated a strong correlation with the zero-order kinetic model ($R^2 = 0.989$), suggesting that the release was concentration-independent and primarily governed by a diffusion-controlled mechanism. Compared to a standard RFN suspension, the SLN formulation exhibited significantly sustained and controlled drug release over the 24-hour period ($^*p < 0.05$), confirming its potential for prolonged therapeutic action.

Table 4: *In-vitro* release of RFN from all developed formulations for 24 hours.

Sr. No.	Formulation code	RFN release after 24 hours	Amount of RFN (µg/mL) release from RFN-EC-SLN after 24 hours
1	F1	84 ± 1.2	420
2	F2	75 ± 1.4	375
3	F3	78 ± 1.6	390
4	F4	87 ± 0.6	435
5	F5	82 ± 1.9	410
6	***F6***	***86 ± 2.4***	***430***
7	F7	75 ± 2.6	375
8	F8	78 ± 2.3	390
9	F9	69 ± 0.7	345
10	F10	72 ± 1.1	360
11	F11	74 ± 1.3	370
12	F12	69 ± 0.9	345
13	F13	76 ± 1.4	380

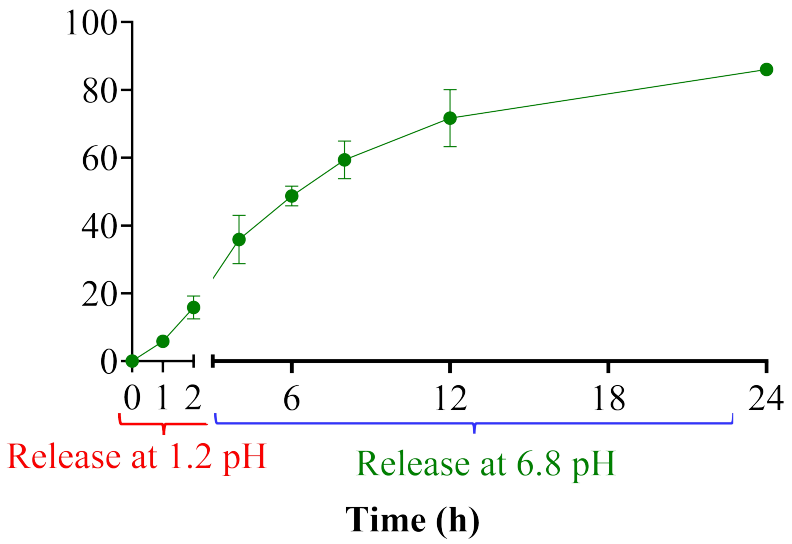

Fig. 8: Cumulative RFN release from RFN-EC-SLN over 24 hours via a dialysis cassette

Table 5: Regression coefficients of different kinetic models applied to the RFN-EC-SLN formulation

Release kinetic models	Formulation
	RFN-EC-SLN (R^2)
Zero-order	0.989
First-order	0.794
Higuchi	0.889
Hixon-Crowell cube root	0.988

Korsmeyer-Peppas n = Release exponent	0.916 (n = 1.801)

Stability Studies:

The optimized RFN-EC-SLN formulation was subjected to accelerated stability testing in compliance with ICH recommendations. Throughout the three-month evaluation, critical parameters remained consistent and within the permissible range. No evidence of instability, including phase separation or visible changes, was detected. The drug content showed negligible variation, with RFN loading maintained at 9.95 ± 0.1% (79.6 ± 2.9%) compared to the initial 10.2 ± 0.2% (82.0 ± 1.6%). These results confirm that the developed formulation possesses robust physical and chemical stability under accelerated storage conditions.

Table 6: Stability Study Data of RFN-EC-SLN

Parameters	**Initial**	**Accelerated Stability (After 3 Months)**
Particle size (nm)	154 ± 2.6	158 ± 4.2
PDI	0.21 ± 0.03	0.24 ± 0.04
Zeta potential (mV)	+17.5 ± 0.04	+17.2 ± 0.08
Phase separation	No	No
Physical appearance	Clear	Clear
pH	6.9 ± 0.2	6.8 ± 0.4
RFN content over the period (%)	10.2 ± 0.2	9.95 ± 0.1

***In-vivo* safety evaluation**

Acute toxicity assessment

The acute safety profile of rifaximin formulations, including oral suspension, rifaximin-loaded solid lipid nanoparticles (RFM-SLN), and intravenous rifaximin solution, was evaluated following a single high-dose administration. The study was conducted in compliance with established ethical and regulatory guidelines. Throughout the 14-day observation period, no mortality, behavioral abnormalities, or clinical signs of toxicity were observed in any treatment group. All animals maintained normal locomotor activity, grooming behavior, respiration, and feeding patterns. The absence of neurological or gastrointestinal disturbances indicates that both the conventional and nanoformulated rifaximin preparations were well tolerated under acute exposure conditions.

Body Weight analysis

Body weight monitoring revealed a consistent and progressive increase across all groups during the study period. No statistically significant differences were detected between treatment groups. Notably, animals receiving the RFM-SLN formulation exhibited slightly greater weight gain compared to the suspension and IV groups, suggesting good gastrointestinal tolerance and absence of metabolic compromise. These findings confirm that the developed nanoformulation did not adversely affect appetite, nutrient utilization, or general physiological status.

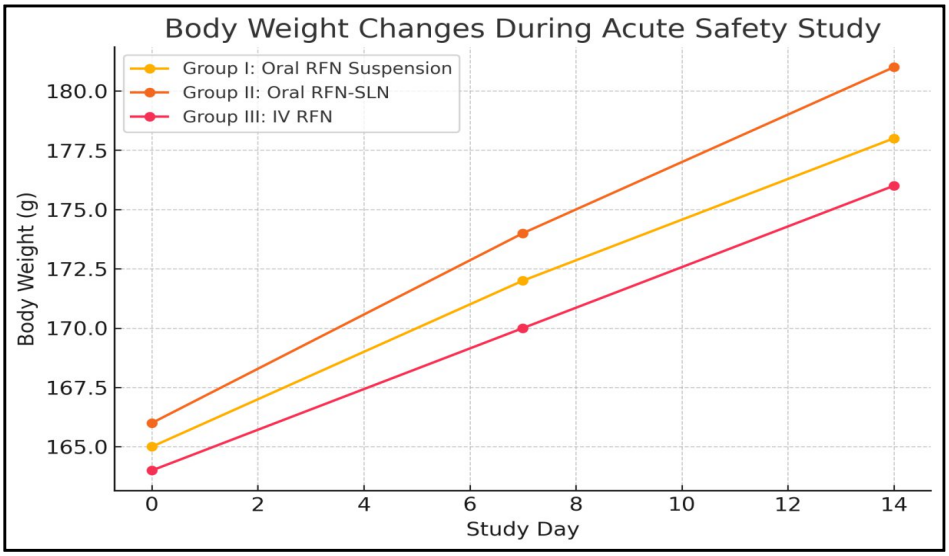

Fig. 9: Body weight changes during acute safety study

Haematological evaluation

Haematological analysis demonstrated that haemoglobin levels, RBC count, WBC count, haematocrit (PCV), platelet count, and differential leukocyte distribution remained within normal physiological ranges in all groups. Statistical comparison showed no significant intergroup differences ($p > 0.05$). The overlapping haematological profiles across treatments indicate that neither the SLN formulation nor the conventional preparations induced hematotoxicity, inflammation, or immunological stress. These results support the haematological safety of the optimized nanoformulation.

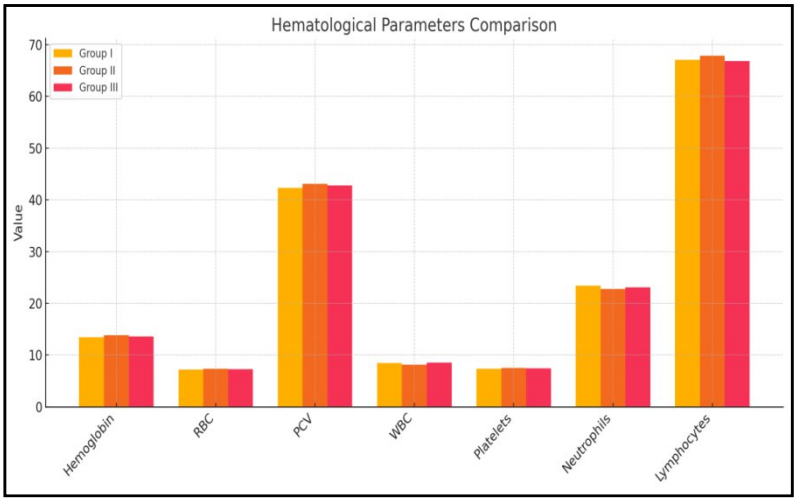

Fig. 10: Hematological parameters of rats after acute safety evaluation

Biochemical assessment of hepatic and renal function

Serum biochemical parameters were analyzed to evaluate potential hepatic and renal toxicity. Liver function markers, including AST, ALT, ALP, and total bilirubin, remained within normal limits in all groups, suggesting the absence of hepatocellular injury or metabolic disturbance. Similarly, renal function indicators such as urea, creatinine, and BUN showed no significant variations among groups ($p > 0.05$), confirming preserved renal function. The comparable biochemical profiles between the SLN-treated animals and controls indicate that the nanoformulation does not exert acute hepatic or nephrotoxic effects.

Collectively, the safety findings demonstrate that the optimized RFM-SLN formulation is well tolerated following single-dose administration and exhibits a safety profile comparable to conventional rifaximin preparations.

***In-vivo* pharmacokinetic evaluation**

Selection of optimized formulation

Among the developed formulations, batch F6 was selected for in vivo pharmacokinetic evaluation based on its superior

physicochemical and biopharmaceutical performance. The formulation exhibited uniform nanoscale particle size, low polydispersity, high entrapment efficiency, sustained drug release, enhanced ex vivo permeation, and marked reduction in efflux ratio. These characteristics suggested improved intestinal absorption and justified its advancement for systemic exposure studies.

Fig. 11: Oral route of drug administration for pharmacokinetic study

Analytical validation for plasma quantification

Plasma rifaximin concentrations were determined using a validated reverse-phase HPLC method. The assay demonstrated excellent linearity over the concentration range of 5–30 µg/mL ($R^2 = 0.9991$), confirming analytical reliability, sensitivity, and compliance with ICH validation standards. The absence of interfering peaks and consistent retention time ensured accurate quantification of pharmacokinetic samples.

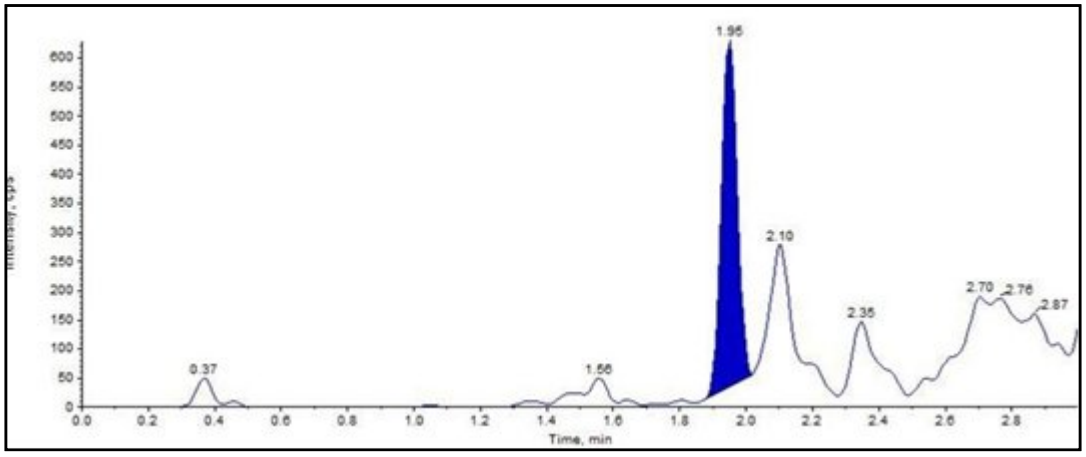

Fig. 12: Representative HPLC Chromatogram of Rifaximin Standard Solution

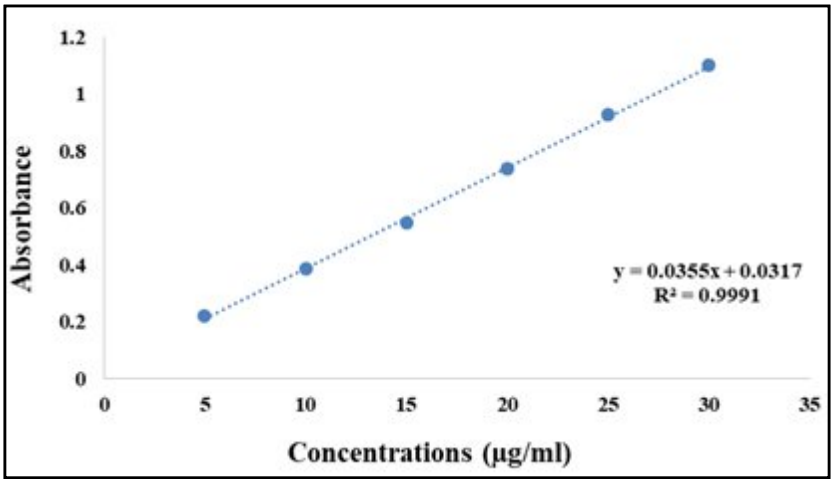

Fig. 13: Calibration curve of Rifaximin

Plasma concentration–time profile

Distinct pharmacokinetic profiles were observed among the three formulations. The intravenous group showed an immediate peak followed by a predictable decline, reflecting rapid systemic distribution and elimination. The oral rifaximin suspension produced comparatively lower plasma concentrations with a faster decline phase, consistent with limited solubility and poor absorption. In contrast, the RFM-SLN formulation generated significantly higher and sustained plasma levels, indicating enhanced absorption and prolonged systemic presence.

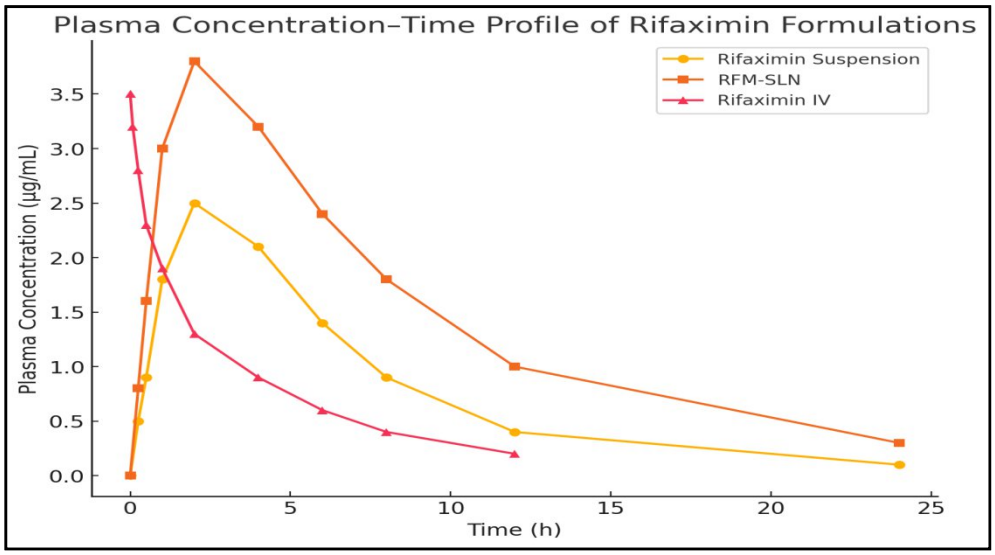

Fig. 14: Plasma Concentration–Time Profile of Rifaximin Formulations

Comparative pharmacokinetic performance

The optimized RFM-SLN formulation demonstrated a marked improvement in pharmacokinetic parameters compared with the conventional suspension. The peak plasma concentration (Cmax) increased from 2.50 µg/mL (suspension) to 3.80 µg/mL, while Tmax decreased from 2 h to 1 h, indicating faster and more efficient absorption. Systemic exposure, reflected by AUC_{0-24} and $AUC_{0-\infty}$, was nearly doubled in the SLN group, confirming significantly enhanced bioavailability. Furthermore, the elimination half-life increased from 3.20 h to 5.10 h, accompanied by a reduced elimination rate constant, suggesting sustained drug release and prolonged circulation time.

The relative bioavailability of the SLN formulation reached 159.3% compared to the conventional suspension, demonstrating a substantial enhancement in oral absorption. These improvements can be attributed to increased solubilization, nanoscale particle size, improved mucosal permeation, reduced P-glycoprotein-mediated efflux, and controlled release from the lipid matrix.

Overall, the pharmacokinetic findings confirm that SLN-based encapsulation effectively overcomes the biopharmaceutical limitations of rifaximin and significantly enhances its oral bioavailability.

CONCLUSION:

The present investigation successfully developed and optimized rifaximin-loaded enteric-coated solid lipid nanoparticles (RFN-EC-SLN) as a strategic approach to overcome the biopharmaceutical limitations associated with BCS Class II drugs. Preformulation studies confirmed the purity, structural integrity, and compatibility of rifaximin with selected excipients. The Quality by Design-based Box–Behnken optimization approach effectively identified lipid concentration as the most critical factor influencing particle size, entrapment efficiency, and drug release behavior.

The optimized formulation (F6) exhibited desirable nanoscale characteristics, including a mean particle size of 154 ± 2.6 nm, low polydispersity index (0.21 ± 0.03), and satisfactory zeta potential (+17.5 ± 0.04 mV), indicating good colloidal stability. High entrapment efficiency (82.0 ± 1.6%) and adequate drug loading (10.2 ± 0.2%) demonstrated efficient incorporation of rifaximin within the lipid matrix. The enteric-coated system showed minimal drug release under gastric conditions and sustained release in intestinal pH, following predominantly zero-order kinetics, thereby confirming controlled and pH-responsive release behavior. Accelerated stability studies further established the formulation's physicochemical robustness.

In vivo safety assessment revealed no mortality, behavioral abnormalities, hematological alterations, or hepatic and renal dysfunction, confirming the tolerability and systemic safety of the nanoformulation. Pharmacokinetic evaluation demonstrated a significant enhancement in oral absorption, with increased Cmax, prolonged half-life, nearly two-fold higher AUC values, and a relative bioavailability of 159.3% compared to conventional rifaximin suspension. The improved systemic exposure can be attributed to enhanced solubilization, nanoscale dispersion, controlled release, and reduced efflux-mediated drug loss.

Overall, the developed RFN-EC-SLN system effectively improved the solubility, stability, intestinal protection, and oral bioavailability of rifaximin. These findings support the potential of enteric-coated solid lipid nanocarriers as a promising delivery platform for enhancing the therapeutic performance of poorly soluble drugs.

CONFLICT OF INTEREST:

The authors declare that there are no conflicts of interest regarding the publication of this research article..

REFERENCES

1. Jain AK, Das M, Swarnakar NK, Jain S. Engineered nanoparticles for oral delivery of poorly soluble drugs: challenges and strategies. Expert Opin Drug Deliv. 2011;8(6):753-766. doi:10.1517/17425247.2011.565743.

2. Ensign LM, Cone R, Hanes J. Oral drug delivery with polymeric nanoparticles: the gastrointestinal mucus barriers. Adv Drug Deliv Rev. 2012;64(6):557-570. doi:10.1016/j.addr.2011.12.009.

3. Mercuri A, Passerini N, Hadrich G. Enteric-coated nanoparticles for oral delivery of lipophilic drugs: challenges and opportunities. Drug Discov Today. 2022;27(1):218-234. doi:10.1016/j.drudis.2021.09.003.

4. Mohanpuria P, Rana NK, Yadav SK. Biosynthesis of nanoparticles: Technological concepts and future applications. Journal of Nanoparticle Research. 2008;10(3):507-517.

5. Hua S. Advances in oral drug delivery for regional targeting in the gastrointestinal tract: influence of physiological, pathophysiological, and pharmaceutical factors. Front Pharmacol. 2020;11:524. doi:10.3389/fphar.2020.00524.

6. Sastry SV, Nyshadham JR, Fix JA. Recent technological advances in oral drug delivery: a review. Pharm Sci Technol Today. 2019;3(4):138-145. doi:10.1016/S1461-5347(00)00247-9.

7. Date AA, Hanes J, Ensign LM. Nanoparticles for oral delivery: design, evaluation, and state-of-the-art. J Control Release. 2016;240:504-526. doi:10.1016/j.jconrel.2016.06.016.

8. Vivero-Escoto JL, Slowing II, Trewyn BG, Lin VS. Mesoporous silica nanoparticles for intracellular controlled drug delivery. Small. 2010;6(18):1952-1967.

9. Mittal G, Sahana DK, Bhardwaj V, Ravi Kumar MNV. Enteric-coated nanoparticles for oral drug delivery. In: Nanoparticulate Drug Delivery Systems. New York: Informa Healthcare; 2012. p. 135-158.

10. Peer D, Karp JM, Hong S, Farokhzad OC, Margalit R, Langer R. Nanocarriers as an emerging platform for cancer therapy. Nature Nanotechnology. 2007;2(12):751-760.

11. Zhang L, Wang S, Zhang M, Sun J. Nanoparticle-based oral drug delivery systems for poorly soluble drugs: design, optimization, and in-vivo evaluation. Int J Pharm. 2020;587:119669. doi:10.1016/j.ijpharm.2020.119669.

12. Patel V, Agrawal YK, Saraf S. Enteric-coated nanoparticles for targeted oral delivery of a poorly water-soluble drug: formulation and pharmacokinetic assessment. Drug Deliv Transl Res. 2019;9(4):789-801. doi:10.1007/s13346-019-00632-3.

13. Garg NK, Singh B, Jain A, Sharma R. Development and optimization of enteric-coated nanoparticles for enhanced oral bioavailability of a BCS Class II drug. J Nanopart Res. 2018;20:156. doi:10.1007/s11051-018-4257-8.

14. Yadav D, Kumar N. Formulation and characterization of enteric-coated polymeric nanoparticles for pH-sensitive delivery of a poorly soluble anticancer drug. AAPS PharmSciTech. 2017;18(6):2187-2196. doi:10.1208/s12249-016-0696-7.

15. Singh A, Bajpai M. Optimization of Eudragit-based enteric nanoparticles for colon-targeted delivery of a hydrophobic drug using Box-Behnken design. Drug Dev Ind Pharm. 2016;42(8):1316-1327. doi:10.3109/03639045.2015.1135939.

16. Khan S, Batchelor H, Hanson P, Perrie Y, Mohammed AR. Enteric-coated nanoparticles for the oral delivery of poorly soluble drugs: formulation and in vitro evaluation. Eur J Pharm Sci. 2021;159:105715. doi:10.1016/j.ejps.2021.105715.

17. Liu Y, Wang Y, Yang J, Zhang H, Gan L. pH-sensitive polymeric nanoparticles for improved oral delivery of a poorly water-soluble drug: design, optimization, and in vivo pharmacokinetics. Int J Nanomedicine. 2020;15:5789-5802. doi:10.2147/IJN.S259525.

18. Sharma G, Thakur K, Raza K, Singh B. Enteric-coated chitosan-based nanoparticles for colon-targeted delivery of cyclosporine A: formulation, optimization, and in vivo evaluation. JMicroencapsul. 2019;36(3):234-246. doi:10.1080/02652048.2019.1622599.

19. Gonçalves LMD, Maestrelli F, Mura P, Cirri M. Development of solid lipid nanoparticles and enteric-coated nanoparticles for oral delivery of a poorly soluble drug: comparative study. Pharm Dev Technol. 2018;23(7):718-726. doi:10.1080/10837450.2017.1362433.

20. Alai MS, Lin WJ, Pingale SS. Application of polymeric nanoparticles and micelles in the delivery of poorly soluble drugs: a review. J Nanosci Nanotechnol. 2017;17(4):2304-2317. doi:10.1166/jnn.2017.12825.

21. Beloqui A, Coco R, Alhouayek M, Solinís MÁ, Rodríguez-Gascón A, Muccioli GG. Budesonide-loaded nanoparticles with pH-sensitive coating for improved mucosal drug delivery in ulcerative colitis. Nanomedicine. 2016;11(6):616-628. doi:10.2217/nnm.15.218.

22. Zhang X, Wu W. Ligand-mediated active targeting for enhanced oral absorption of poorly soluble drugs. Adv Drug Deliv Rev. 2015;95:104-115. doi:10.1016/j.addr.2015.09.004.

23. Taheri A, Almasri R, Wignall A, Schultz HB, Elz AS, Ariaee A, et al. Enhancing the pharmacokinetics of abiraterone acetate through lipid-based formulations: Addressing solubility and food effect challenges. Drug Deliv Transl Res. 2024.

24. Shah S, Famta P, Vambhurkar G, Sharma A, Mourya A, Srinivasarao DA, et al. Exploration of abiraterone acetate-loaded nanostructured lipid carriers for bioavailability improvement and circumvention of fast-fed variability. Drug Deliv Transl Res. 2025;15:1074–1091.

25. Schultz HB, Meola TR, Thomas N, Prestidge CA. Oral formulation strategies to improve the bioavailability and mitigate the food effect of abiraterone acetate. Int J Pharm. 2020;577:119069.

26. Schultz HB, Wignall AD, Thomas N, Prestidge CA. Enhancement of abiraterone acetate oral bioavailability by supersaturated-silica lipid hybrids. Int J Pharm. 2020;582:119264.

27. Larsen AT, Ohlsson AG, Polentarutti B, Barker RA, Phillips AR, Abu-Rmaileh R, et al. Oral bioavailability of cinnarizine in dogs: Relation to SNEDDS droplet size, drug solubility and in vitro precipitation. Eur J Pharm Sci. 2013;48:339–350.

28. Brogmann B, Beckert T. Enteric targeting through enteric coating. Drugs Pharm Sci. 2001;115:1–30.

29. Joyce P, Tan A, Whitby CP, Prestidge CA. The role of porous nanostructure in controlling lipase-mediated digestion of lipid loaded into silica particles. Langmuir. 2014;30:2779–2788.

30. Joyce P, Dening TJ, Gustafsson H, Prestidge CA. Modulating the lipase-mediated bioactivity of particle-lipid conjugates through changes in nanostructure and surface chemistry. Eur J Lipid Sci Technol. 2017;119:1700213.

31. Joyce P, Kempson I, Prestidge CA. QCM-D and ToF-SIMS investigation to deconvolute the relationship between lipid adsorption and orientation on lipase activity. Langmuir. 2015;31:10198–10207.

32. Joyce P, Kempson I, Prestidge CA. Orientating lipase molecules through surface chemical control for enhanced activity: A QCM-D and ToF-SIMS investigation. Colloids Surf B Biointerfaces. 2016;142:173–181.

33. Stappaerts J, Geboers S, Snoeys J, Brouwers J, Tack J, Annaert P, et al. Rapid conversion of the ester prodrug abiraterone acetate results in intestinal supersaturation and enhanced absorption of abiraterone: In vitro, rat in situ and human in vivo studies. Eur J Pharm Biopharm. 2015;90:1–7.

34. Acharya M, Gonzalez M, Mannens G, De Vries R, Lopez C, Griffin T, et al. A phase I, open-label, single-dose, mass balance study of 14C-labeled abiraterone acetate in healthy male subjects. Xenobiotica. 2013;43:379–389.

35. Van Speybroeck M, Mellaerts R, Mols R, Do Thi T, Martens JA, Van Humbeeck J, et al. Enhanced absorption of the poorly soluble drug fenofibrate by tuning its release rate from ordered mesoporous silica. Eur J Pharm Sci.

2010;41:623–630.

36. Patra CN, Priya R, Swain S, Jena GK, Panigrahi KC, Ghose D. Pharmaceutical significance of Eudragit: A review. Future J Pharm Sci. 2017;3:33–45.

37. Nguyen HT, Van Duong T, Taylor LS. Impact of gastric pH variations on the release of amorphous solid dispersion formulations containing a weakly basic drug and enteric polymers. Mol Pharm. 2023;20:1681–1695.

38. Nguyen HT, Van Duong T, Taylor LS. Enteric coating of tablets containing an amorphous solid dispersion of an enteric polymer and a weakly basic drug: A strategy to enhance in vitro release. Int J Pharm. 2023;642:123139.

39. Qin Y, Xiao C, Li X, Huang J, Si L, Sun M. Enteric polymer-based amorphous solid dispersions enhance oral absorption of the weakly basic drug nintedanib via stabilization of supersaturation. Pharmaceutics. 2022;14:1830.

40. Angi R, Jordán T, Basa-Dénes O, Solymosi T, Ötvös Z, Glavinas H, et al. Complexes of abiraterone acetate, process for the preparation thereof and pharmaceutical compositions containing them. US Patent 10,668,016. 2 June 2020.

41. Won JH, Jin M, Na YG, Song B, Yun TS, Hwang YR, et al. A combinative strategy for improving the intestinal stability and cellular absorption of curcumin by enteric coating of optimized nanostructured lipid carriers. J Drug Deliv Sci Technol. 2023;89:105108.

42. Hosny KM. Alendronate sodium as enteric-coated solid lipid nanoparticles: Preparation, optimization, and in vivo evaluation to enhance its oral bioavailability. PLoS One. 2016;11:e0154926.

43. Sahu KK, Kaurav M, Pandey RS. Chylomicron-mimicking solid lipid nanoemulsions encapsulated enteric minicapsules targeted to colon for immunization against hepatitis B. Int Immunopharmacol. 2019;66:317–329.

44. Li C, Zhou K, Chen D, Xu W, Tao Y, Pan Y, et al. Solid lipid nanoparticles with enteric coating for improving stability, palatability, and oral bioavailability of enrofloxacin. Int J Nanomedicine. 2019;14:1619–1631.

45. Liu K, Liu W, Dong Z, Zhang L, Li Q, Zhang R, et al. Translation of ionic liquids to enteric nanoparticles for facilitating oral absorption of cyclosporine A. Bioeng Transl Med. 2023;8:e10405.

46. Joyce P, Allen CJ, Alonso MJ, Ashford M, Bradbury MS, Germain M, et al. A translational framework to deliver nanomedicines to the clinic. Nat Nanotechnol. 2024;19:1597–1611.

47. Hosny KM, Osama A, Al-Abdaly R. Enteric-coated alendronate sodium nanoliposomes: a novel formula to overcome barriers for the treatment of osteoporosis. Expert Opin Drug Deliv. 2013;10(6):741–746. doi:10.1517/17425247.2013.799136.

48. Meyyanathan SN, Muralidharan S, Rajan S, Gopal K, Suresh B. A simple sample preparation with HPLC-UV method for estimation of amlodipine from plasma: Application to bioequivalence study. Open Chem Biomed Methods J. 2008;1:22–27.

49. Valliappan K, Kannan K, Sivakumar T, Manavalan R. Enantiospecific pharmacokinetic studies on ketoprofen in tablet formulation using indirect chiral HPLC analysis. J Appl Biomed. 2006;4:153–161.

50. Teply BA, Tong R, Jeong SY, Luther G, Sherifi I, Yim CH. Charge-coupled polymeric microparticles and micromagnets for modulating the bioavailability of orally delivered macromolecules. Biomaterials. 2008; 29:1216–1223